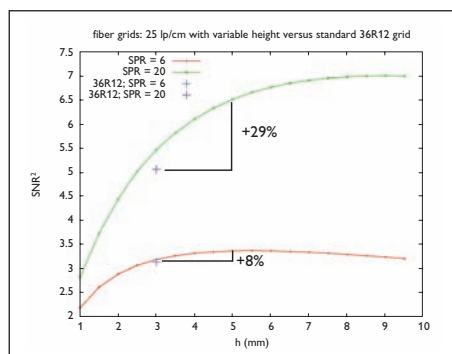


# Improving digital image quality for larger patient sizes without compromises

Christiaan Kok, Technology Physicist Grids  
Smit Röntgen, Best, The Netherlands



In recent years the average patient has increased in weight. It is well-known that an X-ray image of an overweighted or obese patient has a lower image quality than an X-ray image of a standard patient. Due to the fact that the X-rays have to transverse more body mass, the radiologist has to choose a higher kV setting to obtain an image whilst maintaining a reasonable dose and tube load. At higher kV the penetrating power of X-rays increases, but the contrast between different parts of the body decreases. Also the amount of scatter increases very rapidly with increasing body mass, which will further decrease contrast.

For digital imaging systems, the DQE (detective quantum efficiency) is the most important image quality determining factor. The DQE is related to the Signal to Noise Ratio (SNR). If scatter is present in an image, the DQE is reduced.

An improved anti-scatter grid is introduced with better scatter reduction. This new grid improves the imaging system's DQE for high scatter conditions. Therefore the image quality of X-ray images of overweighted patients is significantly improved. The performance for standard patients is not compromised.



# Introduction to X-ray imaging systems

Radiography is the general imaging of body parts by X-ray radiation. A schematic of the imaging setup is given in Figure 1.

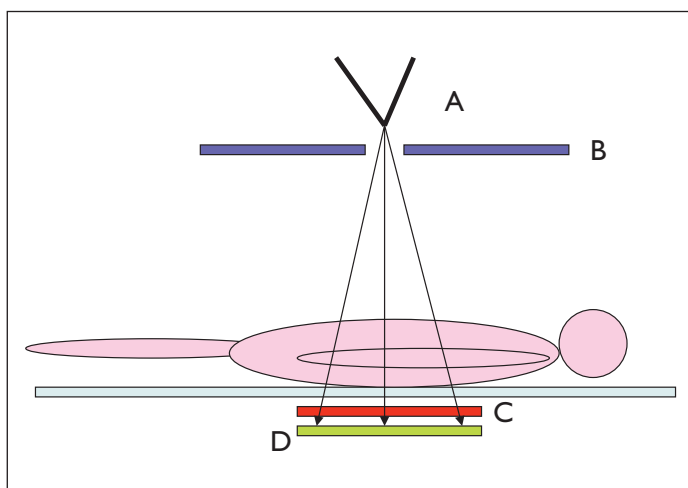


**Figure 1** Schematic of imaging setup (meaning of symbols denoted in main text)

A short description of the main components, denoted by the letters A-D in Figure 1, is now given.

In Figure 1, the symbol A denotes the X-ray source, also called the tube. In the tube a beam of electrons is accelerated to high potential (20–140 kV, denoted as kVp setting) and impinges on a metal disc, the anode. Under this violent bombardment with electrons the metal will emit X-ray radiation, although much of the energy of the electrons is dissipated as heat. The amount of heat which the anode can withstand limits both the current of the electrons and the total amount of X-ray which can be generated. The amount of X-rays is related to the notion of mAs which is the product of the electron current in milliamperes and the time the electron beam is running in seconds. The physics of the X-ray generation process dictates that a broad X-ray spectrum is obtained, meaning that X-rays of many different energies are

produced. In many applications a thin metal sheet (spectral filter) is put in the X-ray beam to preferentially attenuate the low-energy X-rays which are incapable of reaching the X-ray detector but may harm the patient.

The symbol B denotes the next important component of an imaging system: the collimator. A collimator is used to limit the irradiated area on the patient. Since X-ray radiation is detrimental for humans it is necessary to limit the X-ray exposure to only the part of the patient which is of interest.

The letter C denotes the anti-scatter grid, or grid, which will be dealt with in much detail in a later section.

Finally, the letter D denotes the detector, which in most modern systems is a digital flat detector. Most flat detectors have a scintillator material on top of the detector plate which converts the X-rays into visible light. The visible light is detected by the detector plate, which is subdivided into a square pattern of pixels. These pixels each give an output signal proportional to the measured intensity and from these signals a digital image is built [1].

The many peripherals, which are connected to modern imaging systems, are not discussed here, since they have minor relevance for the concepts discussed in this document. A more thorough description of an X-ray system can be found in [2].

# Scatter and noise in X-ray imaging

Scatter is defined as X-ray radiation not emanating from the X-ray source. Most scatter is produced in the patient by a number of physical processes which all produce secondary X-ray radiation propagating in random directions and with energies lower or equal to the primary radiation. Detailed descriptions of the physical processes involved are described in the literature.

To demonstrate the effect of scatter on image quality a simplified model, called a phantom, is depicted in Figure 2. The symbols are familiar from Figure 1, only the grid (C) has been removed for simplicity and the patient is replaced by a phantom (F) comprising a

rectangular slab of material with a sphere shaped feature in dark blue inside. The plastic PMMA is often used as phantom material since its X-ray properties are similar to soft body tissue and the solid material can be easily shaped and handled. For the objects often real bone material or artificial mixtures of metals and plastics are used. In this case the sphere attenuates the X-rays stronger than the surrounding PMMA.

Attenuation of X-rays in materials is governed by the law of Lambert-Beer, which states that the X-ray intensity decays exponentially in the path length ( $x$ ) through the material.

$$I = I_0 \exp(-\mu x)$$

The scaling coefficient,  $\mu$ , is called the linear attenuation coefficient, which describes the strength of attenuation. The  $\mu$  coefficient is depending both on the material as well as the energy of the X-ray radiation. X-ray opaque materials have high  $\mu$  values and X-ray transparent materials have (very) low  $\mu$  values.

For the setup of Figure 2, one can easily simulate images by calculating the attenuation along all possible X-ray trajectories. Such an ideal simulated image of the phantom of Figure 2 is given in Figure 3.

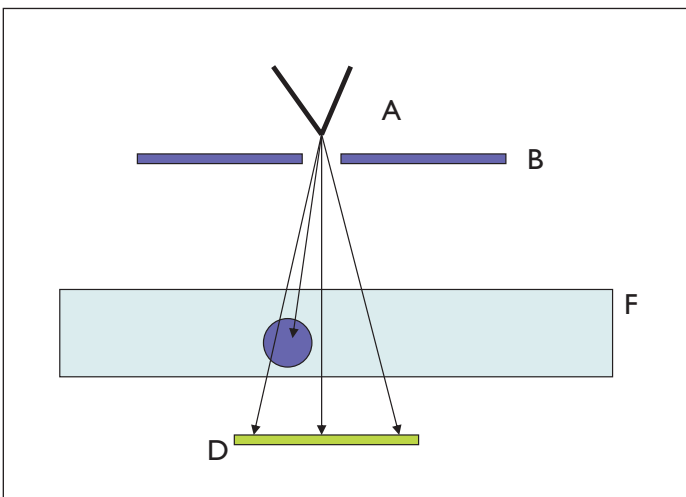


Figure 2 Ideal imaging of a phantom

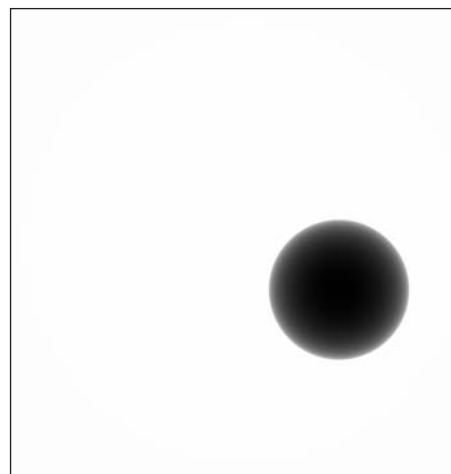
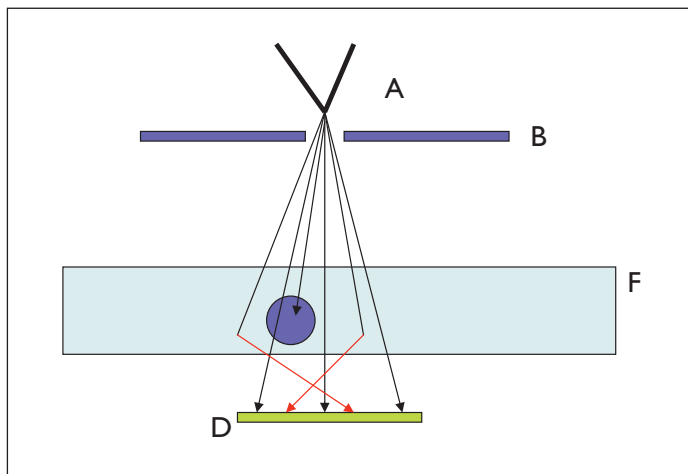


Figure 3 Ideal simulated image

These simulated images should only be used for demonstration purposes since some important image quality limiting features are not incorporated, such as the focal spot size and the influence of the scintillator layer. In an ideal image, which is noise- and scatter-free, the image contrast can be digitally enhanced to any given value. Thus, both low-contrast as well as high-contrast objects can be visualized equally well.

Unfortunately, all real images are influenced by scatter. A schematic of a scatter image setup is given in Figure 4. Some X-rays are deflected away from their original direction by interactions with the phantom material and end up at arbitrary locations on the detector (scattered rays are denoted in red in Figure 4).



**Figure 4** Imaging system with scatter

It is well-known that slab-shaped objects imaged with a wide beam give a circular shaped scatter profile as shown in Figure 5.

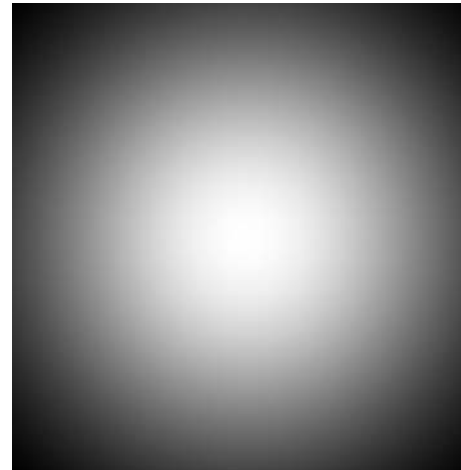


**Figure 5** Ideal scatter profile

For typical radiography conditions, the amount of scatter dominates the primary (=ideal) radiation by a factor varying from 2 to even above 20. Let us assume a common value for the Scatter to Primary Ratio (SPR) of about 6. Adding the images in Figure 3 and 5 scaled by the appropriate values, gives Figure 6.

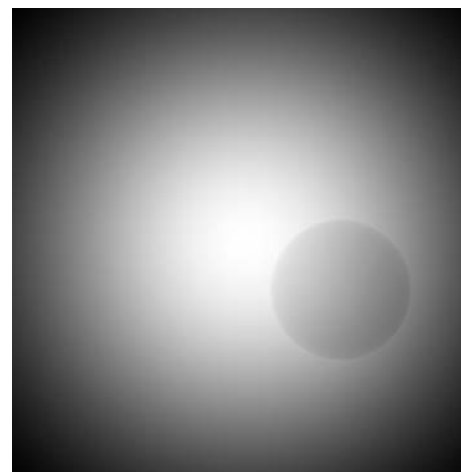


**Figure 6** Noise-free image of feature and scatter

# Scatter and noise in X-ray imaging

One immediately sees that the almost perfect contrast of Figure 3 is deteriorated into a weak contrast in Figure 6 and that the contrast is not constant around the periphery of the sphere. A digital image processing technique called harmonization can be employed to remove for a large part of the additive scatter contribution. This technique is used frequently.

However, scatter is not the only deteriorating effect which must be taken into account. Another important effect is noise. Quantum physics dictates that radiation is transported in quantized energy packets called photons. Due to the limited allowed irradiation of the patient (dose limitation), a limited number of X-ray photons is used to make an image. Therefore, a limited number of such photons reach each detector pixel. These quantized processes are governed by Poisson statistics. This means that the number of photons per pixel varies from pixel to pixel even in homogeneous regions. The amplitude of this variation is of the order of the square root of the average photon count. This variation is called noise.

Noise is often visible as a speckle pattern in the image. The effect is demonstrated in Figures 7, 8 and 9 for the scatter-free image, the scatter image and the total image.

In noisy images, the contrast cannot be arbitrarily increased by simple digital means. An increase in contrast would also lead to an increase in noise and the image would not improve. The effect of noise only decreases if a higher dose is applied, since the signal scales linearly in the dose while the noise scales with a square root in the dose. However, the dose is limited by radiation safety regulations and heat constraints of the tube.

An important point, which must be stressed here, is that harmonization of Figure 9 by digital signal processing can for a large part remove the scatter intensity distribution but it cannot remove the associated noise. Therefore it is always better to remove scatter before it can reach the detector. The removal of the noise associated with scatter (by an anti-scatter grid) will lead to an improvement in the DQE of the system.

The precise details on the influence of scatter on DQE and SNR can be found in the literature [3].

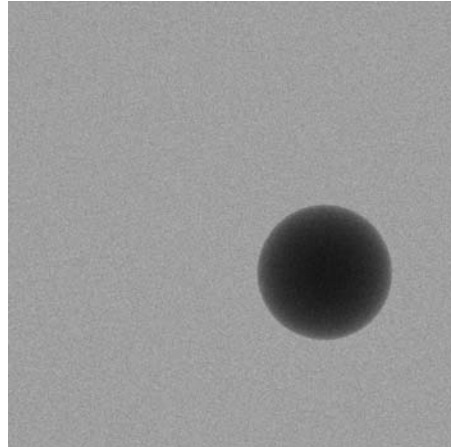


**Figure 7** Scatter-free image with noise



**Figure 8** Scatter profile with noise

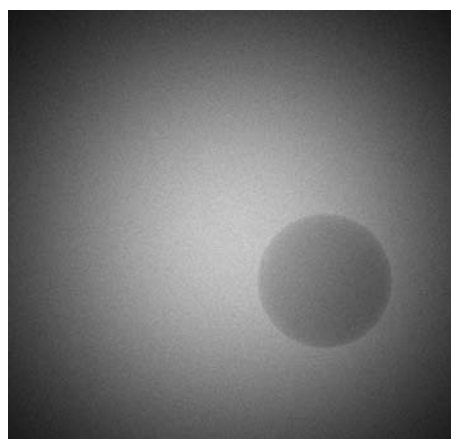


**Figure 9** Total image including both scatter and noise

# Scatter reduction

Several methods exist to prevent the scattered radiation to reach the detector at least to a large part. One method is to increase the distance between the patient and the detector (air gap method) such that most of the highly deflected scatter misses the detector. Several disadvantages of this method include the decreased field-of-view and the decreased efficiency of the X-ray source which increases exposure time and heat load of the X-ray source.

A method which has already a long history in X-ray imaging is the use of a so-called antiscatter grid or grid. Its intended use in X-ray imaging is depicted in Figure 10.

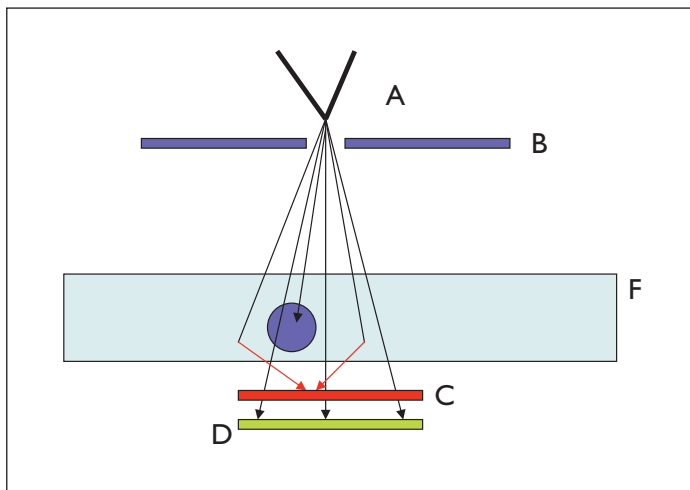


**Figure 10** Function of antiscatter grid in X-ray imaging

The grid (C in Figure 10) blocks preferentially the X-rays which do not emanate directly from the source (red arrows in Figure 10). Several grid types exist, but the most commonly used one is the linear focused grid, which consists of many thin layers of X-ray opaque material interspaced with X-ray transparent layers. A schematic cross section is shown in Figure 11. The label A denotes the X-ray opaque lamellae (in dark grey) and

the label B the X-ray transparent interspacers (light grey). The lamellae are stacked in a slightly tilted way such that they all point towards a line (perpendicular to the paper) on which the X-ray focus lies. The focusing of the grid in Figure 11 is exaggerated.

Typical dimensions for radiography grids are lamella thickness (d) of 0.04 mm, interspacer thickness (D) of 0.2 mm, height (h) of 3 mm, lateral dimensions 450 x 350 mm and a focus distance (f) of 1000 mm.

Most high end grids use lead as lamella material and fiber as interspacer material. Aluminum is also used as interspacer material. Aluminum has the disadvantage of an increased absorption of primary radiation compared to fiber and is therefore more and more replaced with fiber, especially for dose critical applications.

A typical grid consists of more than 1500 carefully stacked lamella. Often the grid is enclosed in a cover for robustness and moisture protection.

Other often used grid-defining parameters can be derived from the geometrical parameters defined above. An important grid parameter is the line rate (N), which is defined as  $N=1/(d+D)$ . The other important parameter is the grid ratio (r), which is defined as  $r=h/D$ .

# Scatter reduction

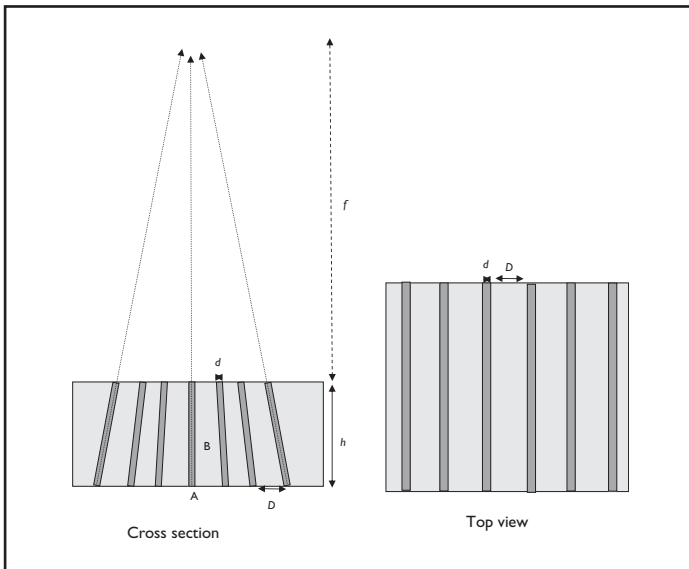


Figure 11 Schematic of focused linear grid

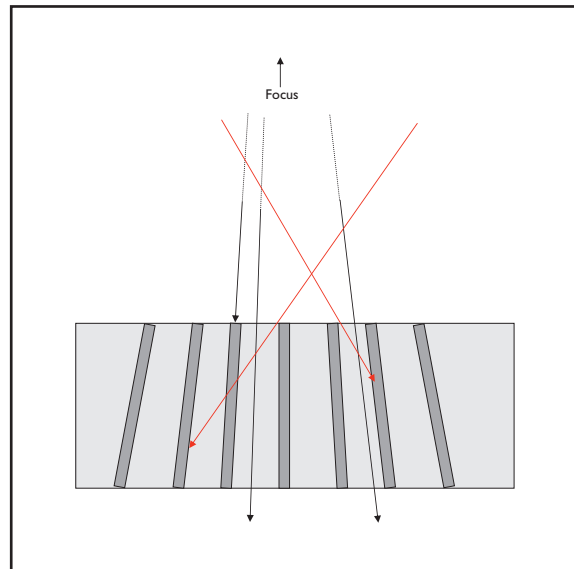


Figure 12 Grid function with scattered radiation

Figure 12 depicts the grid function in more detail. Most of the primary radiation (black arrows) passes unchanged through the grid in between the lead lamellae, although some of the primary radiation is absorbed by the interspacer material. However, the scattered X-rays not emanating directly from the source (red arrows) have a high probability of being absorbed by one or more lead lamellae.

The probability for a primary X-ray to pass through the grid unchanged is denoted by  $T_p$ , the primary transmission coefficient. The probability of a scattered X-ray to pass through the grid unchanged is denoted by  $T_s$ , the scatter transmission coefficient. A proper grid has a high primary transmission coefficient and a low scatter transmission coefficient. A fiber-interspaced grid has a higher transmission of primary radiation than an aluminum-interspaced grid.

The primary and scatter transmission coefficients are functions of imaging conditions and grid parameters. To be able to objectively measure these coefficients, international measurement conditions have been standardized [4].

A disadvantage of using a grid is that a stationary grid casts shadows of the lead lamellae onto the image, which gives rise to artifacts. A way to circumvent this disadvantage was already invented in the 1920's by Bucky and Potter. In their invention, the grid is moved perpendicular to the lamella orientation with a spring system. If the movement during an exposure is over a sufficiently large number of lamellae, the grid artifacts completely disappear. A system in which the grid is moved during exposure is called a bucky system.

A broad overview of topics relating to grid design is given in [6].

# Image quality and grid parameters

To be able to choose the best grid for a given application, an objective criterion for the image quality has to be determined. Many reports in the literature have been written on this subject, but many of those stem from the analog film era [6]. In analog systems a minimum exposure level of the film is important. However this is not so relevant for digital systems, since the signal can be amplified by digital means. For modern digital systems the most important image quality parameter is the Signal-to-Noise Ratio (SNR).

Another concept, which is closely related to the SNR, is the DQE of the imaging system. The exact connection between SNR and DQE is explained in [3]. For the discussion here it is important to know that under certain conditions the improvement in DQE is proportional to the improvement in SNR squared.

We will use the concept of SNR in the following since it can be more intuitively explained and it can be calculated directly from images. The SNR describes the ratio between the measured contrast (signal) and the noise level. In Section 2 we discussed the fact that the noise level in an image is proportional to the square root of the image intensity (scatter plus primary). The contrast is proportional to the primary transmission.

Therefore, we obtain:

$$SNR^2 \propto \frac{Tp^2}{sf \times Tp + (1-sf) \times Ts}$$

where  $sf$  denotes the scatter fraction which is related to the Scatter to Primary Ratio (SPR) by

$$sf = \frac{SPR}{1 + SPR}$$

Much effort has been put in devising models for  $T_s$  as a function of imaging conditions and grid parameters, either by fitting measurement data, geometrical and analytical methods or by computer simulations [5]. General trends can be easily derived. We will state a number of such trends in the following.

The coefficient  $T_p$  can be calculated with high precision for any set of grid parameters since the X-ray trajectories of the primary photons are known. The coefficient  $T_p$  increases when the relative amount of interspacer with respect to the lead lamellae increases and decreases with increasing height of the grid, due to absorption in the interspacer material.

The coefficient  $T_s$  is much more difficult to calculate accurately since their point of origin is randomly distributed in the phantom (or patient). A model for  $T_s$  which is derived from experiments has been devised at Smit-Röntgen. This model has been validated for a wide range of grids at X-ray conditions which are widely used [4]. We substitute the derived functions  $T_p$  and  $T_s$  into the equation stated above for  $SNR^2$  to obtain an equation for  $SNR^2$  as a function of grid parameters under standard conditions.

To investigate the influence of the height on grid performance, the  $SNR^2$  versus the grid height for two different amounts of scatter is plotted in Figure 13 for a grid with 25 line pairs per centimeter and 69 micron thick lead lamellae. The curves show that grids operate optimally at a specific height. This optimum height will shift to higher values if the amount of scatter becomes larger. A current state-of-the-art fiber interspaced grid (36 lp/cm; ratio 12, shorthand to 36R12) has a height

# Image quality and grid parameters

of 3 mm (plus symbols in Figure 13). This grid was designed to be optimal for average-weight patients, with SPR values up to 6.

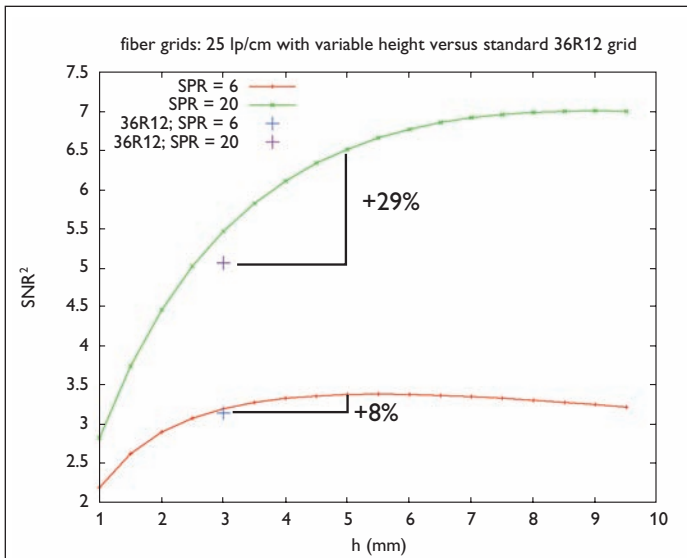


**Figure 13** SNR versus grid height

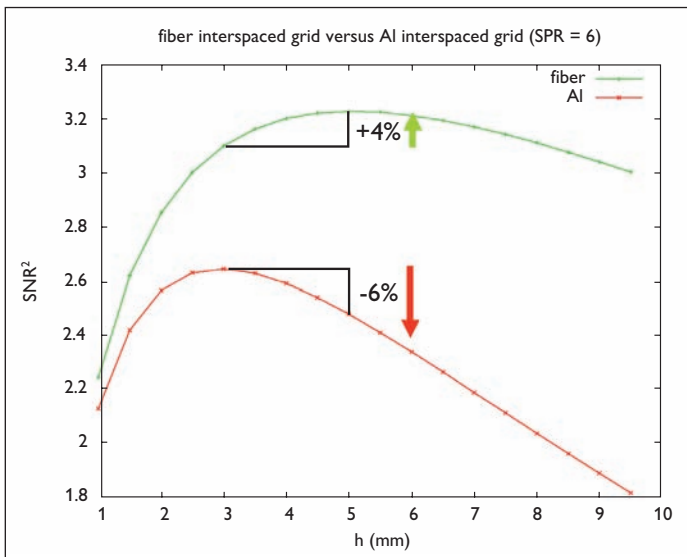
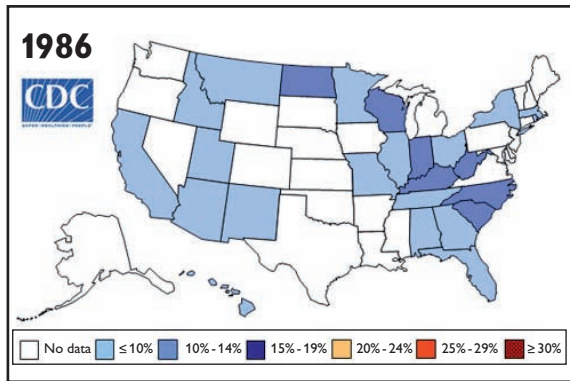


**Figure 14** Performance of fiber grid versus aluminum grid for normal sized patients

A trend, observed in hospitals, is that an increasingly larger fraction of the patient population is obese. For obese patients a large number of examinations will have SPR values easily exceeding 10, sometimes even SPR values above 20 are reached for very large patients. For such examinations, a grid with an increased height will lead to improved image quality. For instance, increasing the height from 3mm to 5mm at an SPR value of 20 leads to an increase in SNR<sup>2</sup> from 5 to 6.5, which is an improvement of more than 25%. It can also be seen that increasing the grid height to 5 mm for normal patients (SPR ≈ 6), the image quality will not be hampered and might even be improved a little. A further increase in height of the grid to values above 5mm would lead to a reduced performance at lower scatter conditions and a reduced flexibility in application due to the increase in ratio.

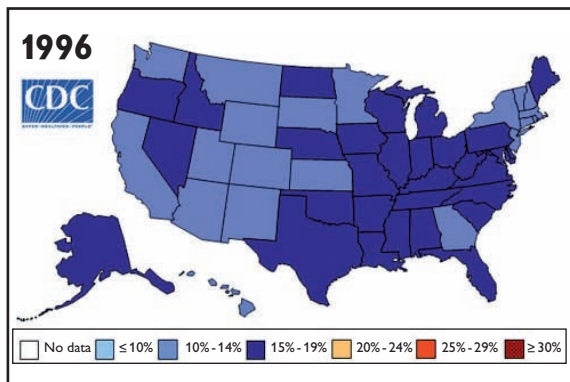
employs aluminum interspacer material. The comparison of the performance of such an aluminum grid with a fiber interspaced grid is depicted in Figure 14 for a normal patient size. From this Figure the great benefit of the fiber interspacer material, especially at increased heights, is obvious. To obtain the same image quality with the aluminum interspaced grid as with the fiber interspaced grid, the dose has to be increased significantly. Therefore, a 5mm high aluminum interspaced grid would have an intolerable impact on dose for normal patients. The conclusion is that increasing the height of an aluminum interspaced grid would not yield the same benefits as with the fiber interspaced grid.

# Obesity

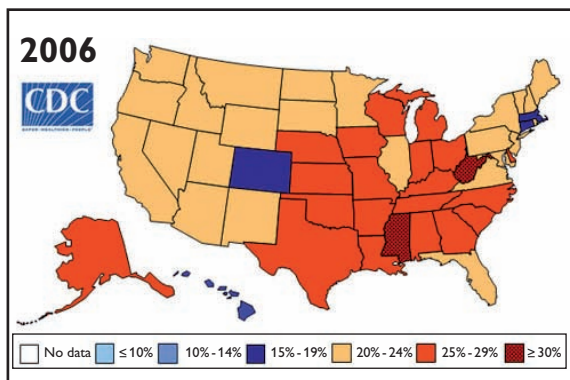


In recent years, especially in the USA, obesity has become a major problem. The CDC estimated in 2004 that approximately 130 million people in the USA were classified as overweight, about 60 million were classified as obese, and 9 million were classified as severely obese (Figure 15).

A measure which is commonly used to measure overweight, is the so-called Body-Mass Index (BMI), which is the mass of a person (in kg) divided by the square of the height of the person (in meter). According to the definitions used by the National Institute of Health, a BMI of over 25 is denoted as overweight, a BMI of over 30 is denoted as obese [7].



Not only the obesity itself poses a health risk for the patient, X-ray imaging, especially of the waist region, is severely hampered by the excess body tissue. To be able to penetrate the increased patient thickness, normally the kV settings of the X-ray tube are increased and higher energy X-rays are generated. These higher energy X-rays penetrate better through the patient. However, the contrast between the different body tissues decreases for these higher energy X-rays leading to a decrease in contrast in the image and lower image quality. Furthermore, the increased path length of the X-rays in the patient lead to a large increase in the amount of scatter, i.e., the SPR increases rapidly. This increase in scatter amount leads to a further decrease in image quality.



Unfortunately, little can be done on the contrast decrease, but the increase in scatter can be successfully battled with an improved anti-scatter grid, leading to an improvement in the system's DQE.

**Figure 15** Obesity in the USA

# A new 5 mm high grid

With the insights of the previous sections, a new 5mm high fiber interspaced grid has been constructed with 25 line pairs per cm and a ratio of 15 (25R15). The grid's form factor has been designed such that it will fit into a normal digital bucky system. The ratio of the new grid is very close to the current ("standard") grid. Therefore, a one to one swap of the current grid with the new grid can be made with no or only minor modifications to the bucky. This swap has no negative effect on image quality for normal patients, but it will improve image quality for the obese patients.

Several experiments have been performed with this grid to compare its performance with the performance of a standard 3 mm high 36 lines/cm ratio 12 (36R12) grid.

## Low contrast measurements

A common and easy quantification procedure is the low contrast measurement where a small object of low contrast is placed on top of a thick and large homogeneous object (Figure 16). From the obtained image, one can measure the average difference in signal strength between the low contrast object and the background. This difference is compared to the standard

deviation of background signal (noise level). Dividing both numbers gives an indication of the Signal to Noise Ratio. These measurements were performed with approximately 1cm of water thickness on top of a pile of PMMA plates with thicknesses of 20 cm, 30 cm and 40 cm. The measured differences in intensity values and standard deviations are tabulated in Table 1.

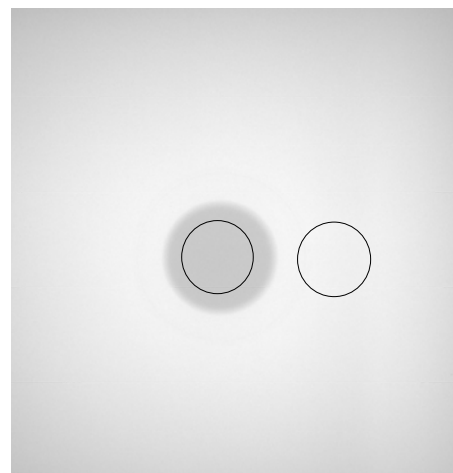
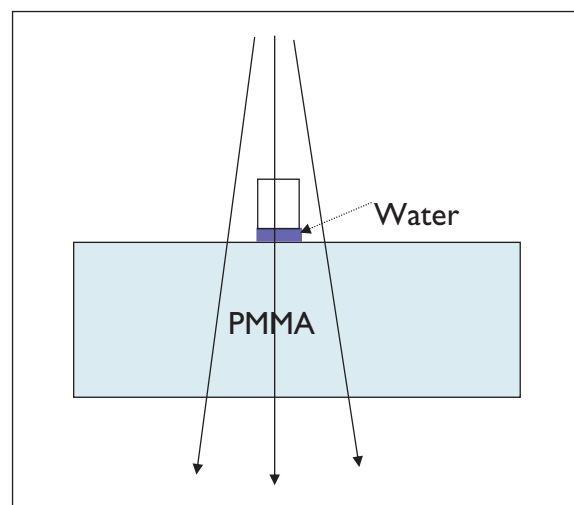


**Figure 16** Low contrast measurements; circles are Regions of Interest

thickness	grid	height	kVp	mAs	Signal difference	SNR	Improvement
20 cm	36R12	3 mm	70	50	256	30.4	+ 6 %
20 cm	25R15	5 mm	70	50	248	32.3	
30 cm	36R12	3 mm	90	80	96.3	12.9	+ 28 %
30 cm	25R15	5 mm	90	80	101	16.6	
40 cm	36R12	3 mm	110	160	40.6	5.48	+ 68 %
40 cm	25R15	5 mm	110	160	49.1	9.25	

**Table 1** Low contrast measurements

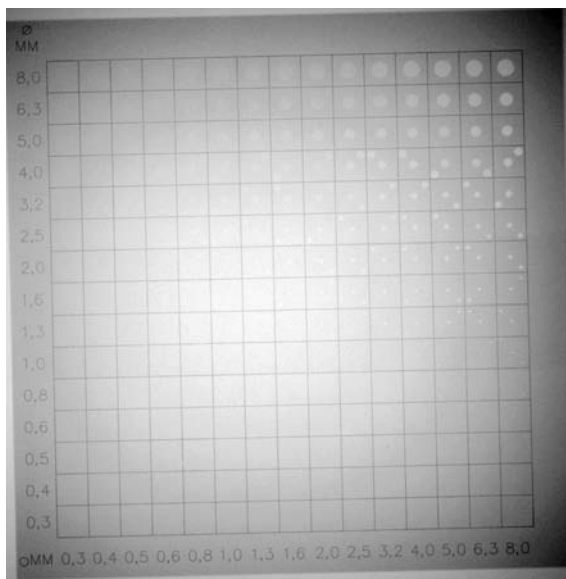
One can see clearly from the rightmost column in Table 1, that the signal to noise ratio is increased by employing the new grid at constant kVp and mAs settings compared to the current 36R12 grid. Especially in the case of 40 cm PMMA, the SNR value increases tremendously. This measured increase in SNR performance is even higher than we expect from the theoretical treatment of section 4.

The DQE improvement is the square of the SNR improvement [3] and therefore almost a factor of three is gained.

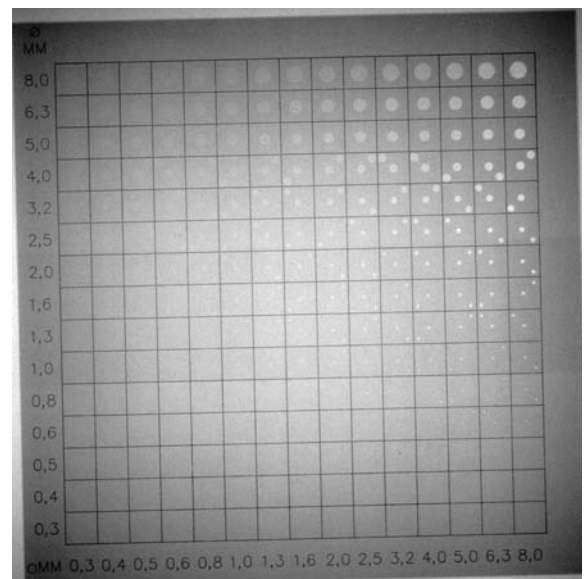
## CDRAD measurements

A different method to quantify grid performance involves the CDRAD phantom [8]. The CDRAD phantom consists of a thin PMMA plate with holes of various sizes and depths, such that both the Contrast (different hole depths) and the Detail (different hole sizes) performance can be measured.

To generate a realistic amount of scatter, 30 cm of PMMA was added above the CDRAD phantom. The leftmost image in Figure 17 is made with a standard 36R12 (3 mm high) grid; the rightmost image in Figure 17 is made with the new 25R15 (5 mm high) grid, under identical conditions (90 kV, 200 mAs,  $SPR \approx 10$ ). It is immediately obvious that the rightmost image suffers much less from the scatter background and more details can be discerned, especially in the center of the image. The software provided by the phantom manufacturer is able to quantify this improvement in image quality into a single number ( $IQ_{inv}$ , [8]). A higher number denotes a better image. For the 36R12 grid the software determines  $IQ_{inv}$  to be 3.67, for the 25R15 grid an  $IQ_{inv}$  of 4.19 is found.



Standard grid



New grid

**Figure 17** CDRAD phantom images

# A new 5 mm high grid



**Figure 18** Body phantom images at equal dose settings

## Body phantom measurements

To investigate the effect the new grid would have on a clinical image, body phantom images were made. The body phantom is an artificial chest of approximately 20 cm thickness, filled with bones, “tissue” and air.

The body phantom was thickened with the addition of 15 cm of PMMA. The maximum total thickness was 35 cm. The image with the standard (36R12) grid was

imaged at 80 kV because at a higher kVp setting the image contrast becomes intolerably compromised. When the new 25R15 grid is used, due to the reduced influence of scatter and improved contrast, a higher kVp setting of 90 kV can be chosen at a lower mAs setting to have equal dose to the patient and as can be seen from the right image in Figure 18, the image quality is improved, especially in the lower abdominal region.

## Clinical testing

The new 25R15 grid is currently under clinical testing at a leading medical institute. A detailed report will be published in a leading medical journal.

# Summary and conclusions

In this document an overview has been given on all the major components of a general radiography X-ray system. The influence of scatter and noise on image quality has been discussed and the influence of an antiscatter grid is shown. A simple model has been derived for the image quality as a function of grid parameters. From this model it is shown that at high scatter conditions a higher grid is beneficial.

Calculations show also the **large benefit of the fiber interspaced grid** with respect to the aluminum interspaced grid, especially for higher grids.

A grid with **increased height** of 5 mm has been made and its performance under several experimental conditions has been tested and compared to the performance of a normal grid. The conclusion from

these experiments was that an **improved image** is obtained by using a grid with increased height for patients which have above average weight. The improvement stems from the increased efficiency of removing scatter at **equal dose**. The improvement in SNR values was shown to be 69 % in some cases. An increase in SNR value leads to an increase in the system's DQE up to a factor of three.

For normal sized patients it is shown that the image quality is not compromised.

The grid is designed such that it fits into a normal digital bucky system.

## References

[1] "Flat detectors and their clinical applications", Spahn, Eur. Radiol. 15 (2005)

[2] Handbook of medical imaging Volume 1: Physics and psychophysics, Beutel et al, SPIE Press, Bellingham WA (2000).

[3] "Generalizing the MTF and DQE to include x-ray scatter and focal spot unsharpness: Application to a new microangiographic system", Kyprianou et al, Med. Phys. 32 (2005)

[4] IEC 60627, IEC, Geneva (2001)

[5] "A detailed experimental and theoretical comparison of the angular and energy dependencies of grid transmission", Bernstein et al, Med. Phys. 10 (1983)

[6] "Analysis of secondary screening with special reference to grids for abdominal radiography", Strid, Acta Radiologica Supplement 351, Stockholm 1976

[7] <http://www.cdc.gov/nccdphp/dnpa/obesity/defining.htm>

[8] <http://www.artinis.com>



All rights are reserved. Reproduction in whole or in part is prohibited without the prior written consent of the copyright holder.

Dunlee reserves the right to make changes in specification and/or to discontinue any product at any time without notice or obligation and will not be liable for any consequences resulting from the use of this publication. Dunlee is part of Philips Healthcare.

Printed in Germany: 4512 008 01281/740 \* FEB 2008

Smit Röntgen grids are exclusively available through Dunlee.

Contact worldwide

**Dunlee**

Postbox 218

5600 MD Eindhoven

The Netherlands

Tel: +31 4027 62707

Fax: +31 4027 62478

[www.dunlee.com](http://www.dunlee.com)